Journal of Alloys and Compounds 480 (2009) 369–375

Contents lists available at ScienceDirect

Journal of Alloys and Compounds

journal homepage: www.elsevier.com/locate/jallcom

Combustion synthesis of Al–Cr preforms activated in microwave field

Krzysztof Naplocha*, Kazimierz Granat

Institute of Production Engineering and Automation, Technical University of Wroclaw, ul. Łukasiewicza 5, 50-371 Wroclaw, Poland

ARTICLE INFO

Article history:
Received 5 November 2008
Received in revised form 10 February 2009
Accepted 14 February 2009
Available online 4 March 2009

Keywords:
Composite
SHS
Microwave
Preform
Al–Cr

ABSTRACT

A method of manufacturing porous preforms of intermetallic Al–Cr compounds intended for local reinforcement of composite materials was developed. Cylindrical specimens, cold pressed of powdered Al and Cr mixture with stoichiometric ratio 7:1, 4:1, 9:4 and granularity −10, −44, −74 μm were combusted in a microwave field. Microwave energy was transferred from a magnetron via a standard waveguide and focused by a tuner on the specimen under argon shield. After synthesis initiation (microwave-activated combustion synthesis = MACS), the microwave field was turned off and the reaction comprised the entire specimen. Analysis of the synthesis course on the ground of temperature diagrams revealed that the reaction temperature increased with increasing Cr content, more energy was released in shorter time and other phase transitions occurred.

The obtained XRD patterns showed that the reaction proceeded between solid Cr and liquid Al to create intermetallic phases with residue of starting and transient phases. Microscopic examination of fractures revealed porous structure of the preforms with rounded Al–Cr precipitates covered with tiny cuboid particles. EDS analysis discovered reaction zones around partially reacted Cr particles. A distinct envelope of Al_9Cr_4 on Cr particle was next enclosed with a layer of Al_4Cr compound. Following the reaction progress, pure chromium slowly passed to the envelope that finally disappeared. Selected specimens with uniform structure and sufficient interconnected porosity were subject to infiltration with liquid aluminum alloy. The castings were reinforced by intermetallic structures using the direct-squeeze casting method and typical process parameters.

1. Introduction

Nowadays, the most promising and economic method of manufacturing intermetallic compounds is the self-propagating high temperature synthesis (SHS) with local ignition or volume combustion (VC). It has reached several variations with common advantages like low energy consumption, high product purity and possibility of manufacturing phases with any size and shape. Its disadvantages include porosity and difficulty at maintaining or controlling the synthesis propagation. The synthesis course is usually affected by form of the substrates, their morphology, stoichiometric ratio, bulk density, ignition technology and the amount of energy released during the exothermic reaction. Normally, ignition is initiated by an incandescent filament, laser beam or electric arc, which leads to a rapid temperature rise up to T_m and to the wave propagation usually in one direction. If the criterion T_{ad} (adiabatic temperature) >1800 K [1,2] is not met and energy released in the combustion zone (10–50 μm) is insufficient to initiate the reaction in front of the propagation wave, the synthesis reaction will require supporting by e.g. gas flow [3], electric current [4] or microwave heating that is currently of the greatest interest.

Basic mechanism of the microwave energy variations (electromagnetic radiation with frequency 2.45 or 5.8 GHz) is the so-called dipole friction. In the case of reflecting materials, usually metals, the phenomenon of current flow and the releasing thermal energy adequate to the metal resistance are also important [5,6]. In the most recent researches of multicomponent materials like hybrid materials [7,8], attention is drawn to the so-called microwave effect occurring in the areas where dielectric properties change abruptly.

At present, methods of bonding ceramics with metals or metals with metals are known [9,10]. An important role in this respect is played by additives that support heating and absorb microwave energy to a higher extent, as well as by applied gas atmosphere. In the case of such materials, very good results are obtained by hybrid heating [11]. At the same time, traditional heating is applied, leading to increase and stabilisation of the loss factor, as well as microwave heating that intensifies the whole process.

Combining the SHS processes with microwave heating induces many new phenomena and enables manufacturing special materials. Microwave heating significantly changes typical regularities of the SHS process. Important is not exactly the bulk density, but rather proper matching the components of the mixture and

* Corresponding author. Tel.: +48 71 3204236.
E-mail address: krzysztof.naplocha@pwr.wroc.pl (K. Naplocha).

0925-8388/$ – see front matter © 2009 Elsevier B.V. All rights reserved.
doi:10.1016/j.jallcom.2009.02.085

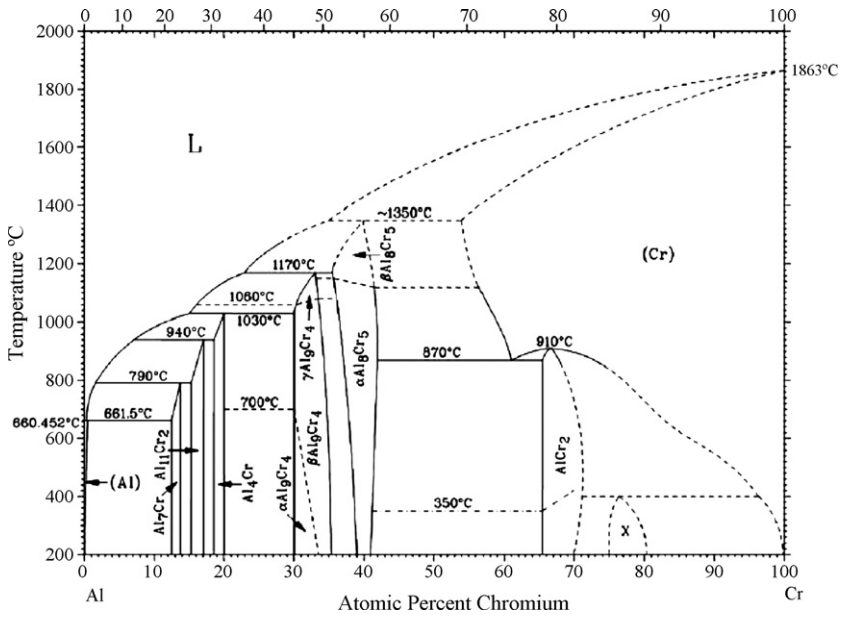

Fig. 1. Al–Cr phase diagram from [14].

creating possibly largest number of contacts [12]. Microwaves increase the temperature growth velocity and thus reduce the number of transition phases [4]. The relatively easy plasma generation of a neutral gas (Ar) can be perfectly used for synthesising non-tractable chemical compounds. Unfortunately, hot spots [4] and substantial stresses [8] can also happen under microwaves. In such cases, it is recommended to displace the material in the microwave field or to break the magnetron supply [13].

In the presented work, the microwave-activated combustion synthesis (MACS) was used for manufacturing porous preforms of Al–Cr compounds. In the two-component Al–Cr system (Fig. 1), with increasing Cr content and temperature (to some degree), the following intermetallic compounds are present: Al_7Cr (or $Al_{13}Cr_2$), $Al_{11}Cr_2$ (or Al_5Cr), Al_4Cr, Al_9Cr_4, Al_8Cr_5 and $AlCr_2$ [14–16]. Using these compounds for reinforcing the aluminum matrix it is possible to increase strength and hardness even at 5% Cr [17]. Usually, these materials are applied in the parts working at high temperatures. At 5–7% Cr already, a tight passivating barrier is created in the aluminum alloy, which rises its corrosion and oxidation resistance at elevated temperatures [18]. This is why these materials are applied in manufacture of gas turbine blades. A similar result can be reached by creating amorphous coatings with e.g. 18% Cr on aluminum parts [19]. Unfortunately, these compounds can also demonstrate low resistance to brittle cracking [20] and then it is recommended to introduce other components, as was done in [21] by adding Ni.

Using combustion synthesis for creating porous structures of these compounds permits obtaining a wide range of functional materials with exceptional morphology. The synthesis course and its initiation possibility for the Al–Cr system are conditioned by energy balance including the reaction enthalpy (Table 1).

The general formula for enthalpy of the SHS reaction initiated at T_{ig} is as follows:

$$-(\Delta H_s + \Delta H_p) = \Delta H_{ign}, \quad (1)$$

where ΔH_s and ΔH_p are parts of enthalpy used for heating substrates and products, correspondingly.

On the ground of few data and relationships described in [14,22,23], an enthalpy diagram of the substrates and the reaction products of the Al_9Cr_4 compound was determined, see Fig. 2. A preliminary analysis of the diagram leads to the following conclusions:

1. Ignition of a sample at $T_0 = 298$ K is impossible due to low energetic yield of the reaction, $\Delta H_{298} < \Delta H_s$, see line I in Fig. 2.
2. Assuming very low thermal losses, i.e. $\Delta Q \rightarrow 0$, and the registered maximum reaction temperature of 1243 K, the preliminary heating temperature to ensure the self-sustaining synthesis course is ca. 750 K, see line II in Fig. 2.
3. If the sample is preliminarily heated-up to the aluminum melting point of 933 K, the maximum reaction temperature can reach 1400 K, see line III in Fig. 2.

At the final research stage, an attempt was made to infiltrate the preforms with aluminum casting alloy by direct-squeeze casting. Natural brittleness of intermetallic compounds composing the preforms should be reduced and the locally reinforced casting would reach new physical properties. Microstructure observations of the obtained composites revealed satisfactory uniformity

Table 1
Formation enthalpy of intermetallic compounds in the Al–Cr system.

Phase	ΔH_T [kJ/mol at.]	Determined at T [K]	Ref.
Al_7Cr	13.4	298	[21]
	13.4	983 solid Al + solid Cr (s-s)	[21]
	22.6	983 liquid Al + solid Cr (l-s)	[21]
$Al_{13}Cr_2$	13.0	298	[22]
$Al_{11}Cr_2$	13.0	298	[22]
	13.1	298	[21]
	9.9	1116 s-s	[21]
	17.4	1116 l-s	[21]
Al_4Cr	17.0	298	[22]
	17.2	298	[21]
	16.8	1194 s-s	[21]
	24.8	1194 l-s	[21]
Al_9Cr_4	16.0	298	[22]
	15.8	298	[21]
	17.8	1213 s-s	[21]
	24.8	1213 l-s	[21]
Al_8Cr_5	15.0	298	[22]
	15.1	298	[21]
	17.7	1283 s-s	[21]
	23.7	1283 l-s	[21]
$AlCr_2$	11.0	298	[22]

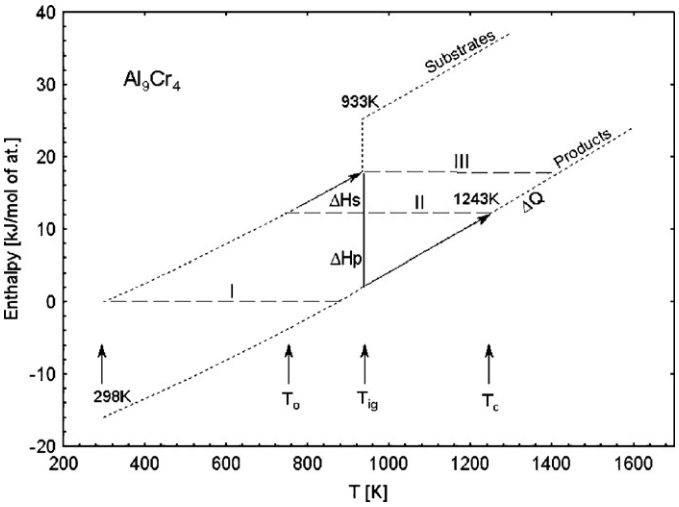

Fig. 2. Enthalpy changes with temperature for substrates (9Al + 4Cr) and product (Al_9Cr_4).

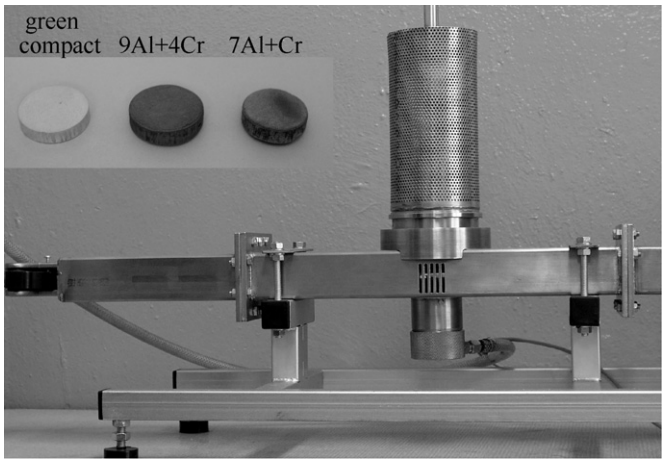

Fig. 3. View of the reactor with heating chamber for combustion synthesis, in the corner green compact and porous products from two mixtures of Al:Cr powder with stoichiometric ratio 9:4 and 7:1.

with no larger defects and segregation. Elimination of porosity in some samples would require further works on selecting infiltration parameters.

2. Materials and methodology

Preparation of the materials consisted of 3 basic stages. At first, proper quantities of Al and Cr powders were mixed in stoichiometric ratios 7:1, 4:1 and 9:4. When fixing the ratios, potential compounds described in the two-component Al–Cr system were considered. Metallic powders produced by AlfaAesar are characterised by well homogeneous granularity and chemical composition. The samples examined in this work were prepared of one kind of Al powder (99.9% Al, −325 mesh) and three kinds of Cr powder (99.5% Cr, −200, −325 mesh and 10 μm). Of these powders, 9 types of samples were prepared, as listed in Table 2 together with the simplifying symbols. The numbers before brackets indicate stoichiometric ratio and those in brackets – Cr granularity.

In order to prepare cylindrical samples dia. 23 mm and 4.5 mm high, the powder mixture was cold pressed at 484 MPa. Structure of the obtained preforms was uniform, with no segregation and agglomeration.

The combustion synthesis was carried out in a specially designed combustion head with a quartz tube filled with argon atmosphere, see Fig. 3. Installing the head in a standard waveguide ended with a tuner enabled tuning and focusing the field in the heating chamber. A typical magnetron was used in the equipment, with a power supply unit adjustable from 0 to 900 W. A few seconds after starting-up, the magnetron was supplied with constant power of 240 W. After the sample was heated up, just before ignition and rapid temperature jump, electric supply was disconnected by pyrometer sensor control at 880 K.

Temperature was measured basically with a pyrometer Raytek, model Marathon MM, with temperature range from 540 to 3000 °C. Diameter of the measuring spot was ca. 0.6 mm. The sample, partially insulated with Al_2O_3 blanket, touched a SiC washer strongly absorbing microwaves. Temperature was measured on the opposite side of the sample with respect to the ignition point. After the reaction, dimensions of the sample were proportionally larger in the entire volume, the sample gained interconnected porosity and strength dependent on the stoichiometric ratio. In most cases, properties of such obtained structures indicated that their infiltration with molten metal was possible. The structures were examined with an optical microscope JEOL JSM-5800LV with an attachment for chemical analysis EDS.

Phase identification was carried out using an X-ray diffractometer (XRD) Rigaku Ultima IV with Cu Ka radiation at 40 kV and 40 mA.

The last step of the developed process was infiltrating the preforms by direct-squeeze casting. The process parameters were close to those applied in the previous years [24], with relatively low infiltration pressure of 40 MPa. Although the preliminary tests were carried out with no greater difficulties, the process should be improved in order to eliminate microporosity in the structure of some composites.

Table 2
Types of samples together with the simplifying symbols.

Cr granularity/mesh	Stoichiometric ratio Al:Cr		
	7:1	4:1	9:4
−10 μm	7(−10 μm)	4(−10 μm)	9(−10 μm)
−44 μm/−325	7(−44 μm)	4(−44 μm)	9(−44 μm)
−74 μm/−200	7(−74 μm)	4(−74 μm)	9(−74 μm)

3. Examination results

Recording and analysing temperature of a sample in the synthesis zone permits determining basic process parameters and thermodynamic properties of the system. In nearly all the tests, the material was heated to the initial temperature of 880 K. The reaction was initiated at a place distant from the measurement point, so the ignition temperature was not determined exactly. Course of the synthesis and temperature of the initiating absorber indicate that the temperature is higher than aluminum melting point. It is only proper overheating of the sample and obtaining local pre-melting of aluminum powder that allows free progress of the reaction in the entire sample volume. Thus, the melting point quoted in literature [4,25] as the ignition temperature in aluminum-based systems is a minimum value and can be insufficient. In the performed tests, on the contrary to the literature data [1–3], no significant effect of the components stoichiometric ratio, their granularity or the sample size on the ignition nature and temperature was observed. However, distinct differences were observed in the reaction velocity, maximum temperature, product morphology and synthesis stages. Considering possible compounds of the Al–Cr system, the highest synthesis temperature occurred in those with larger Cr quantity, and so with more balanced atomic ratio (Al_9Cr_4). For the samples 7Al + Cr, 4Al + Cr and 9Al + 4Cr, these temperatures were included, respectively, in the ranges of 1028–1057 K, 1112–1150 K

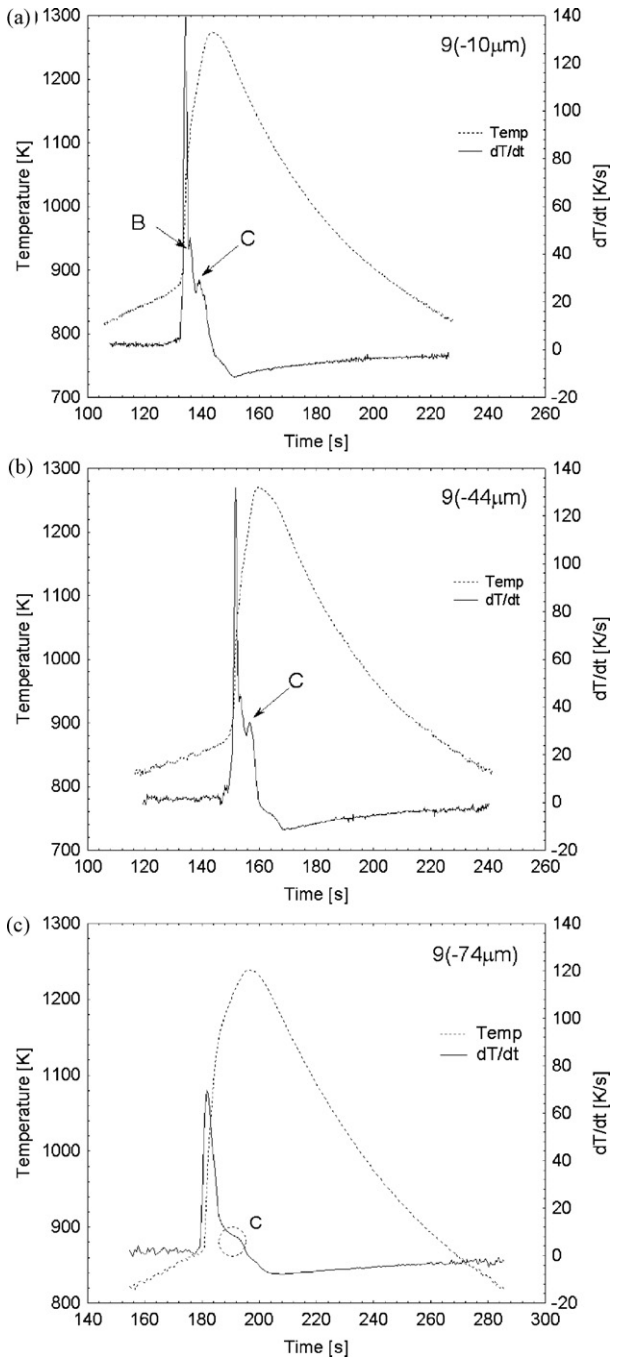

Fig. 4. Temperature profiles and their differentials for 9Al + 4Cr samples with granularity of Cr particles: −10 μm (a), −44 μm (b) and −74 μm (c). Granularity of Al particles for all samples is −44 μm. Phase transformations are: $L + Al_7Cr \rightarrow L + Al_{11}Cr_2$ at B and $L + Al_{11}Cr_2 \rightarrow L + Al_4Cr$ at C.

and 1238–1274 K, see Figs. 4 and 5. It can be read from the diagram that the maximum temperature differentials are within 920–950 K, irrespective of a kind of the sample and its chemical composition. This can suggest that maximum reaction velocity is close to aluminum melting point of 933 K with the presence of liquid phase and thus increased diffusion of elements.

Analysis of transient temperature fluctuations permits specifying possible phase transformations during synthesis progress. In Fig. 4, the point B recorded for the sample 9(−10 μm) at 1074–1093 K evidences the peritectic transformation $L + Al_7Cr \rightarrow L + Al_{11}Cr_2$ that appears in the phase diagram at 1063 K. The next peritectic transformation $L + Al_{11}Cr_2 \rightarrow L + Al_4Cr$ is recorded at

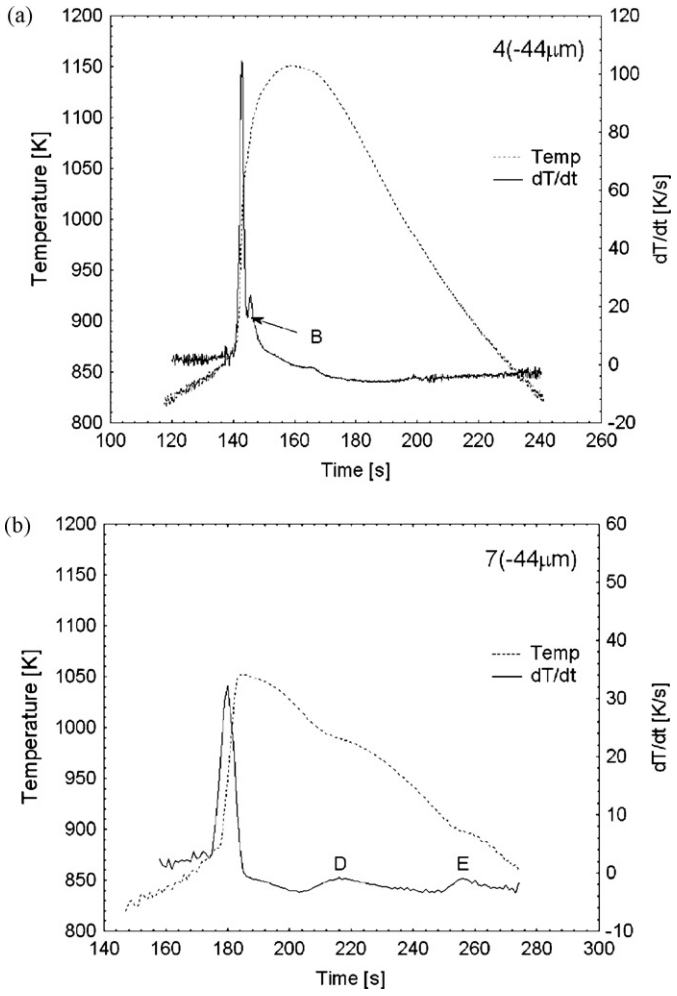

Fig. 5. Temperature profiles and their differentials for 4Al + Cr samples (a) and 7Al + Cr (b). Identical granularity of Cr and Al particles is −44 μm. Phase transformations are: $L + Al_{11}Cr_2 \rightarrow L + Al_7Cr$ at D and $L + Al_7Cr \rightarrow \alpha + Al_7Cr$ at E.

1163–1198 K and marked as C (at 1213 K in the phase diagram). This is clearly visible for almost all the samples, although the temperature peaks get smaller with increasing size of Cr particles. This could result from longer reaction time and impossible recording. The XRD patterns for the 9Al + 4Cr samples, irrespective of Cr particle size, were almost identical. Only the samples based of the coarsest Cr particles (−74 μm) revealed slightly more intensive peaks proving the presence of residual Cr. However, it can be ascertained that phase compositions of the structures created from the 9Al + 4Cr mixture with various powder granularities are nearly identical.

Change of chemical composition leads to a different reaction intensity and lower synthesis temperature. Decreasing the Cr content reduces the maximum reaction temperature below the temperature "C". However, it is still possible to notice the "B" reaction at 1053–1059 K on the temperature profiles for the 4Al + Cr samples (Fig. 5a). Therefore, for both the 9Al + 4Cr and 4Al + Cr samples, the recorded peaks "B" indicate that synthesis begins with forming the Al_7Cr compound. This is also confirmed by analysis of reaction enthalpy values based on an EHF (effective heat formation) model [26–28] that considers minimum reaction enthalpy and the lowest liquidus temperature. Analysed an effective heat formation $\Delta H'$ is defined as: $\Delta H' = \Delta H^0 * C'/C$ where C' is the effective concentration limiting element and C is compound concentration limiting element. Graphic representation of $\Delta H'$ is diagram constructed by plotting the heat of formation, ΔH^0, of each compound at its compositional concentration, expressed in kJ/mol of atoms. Next

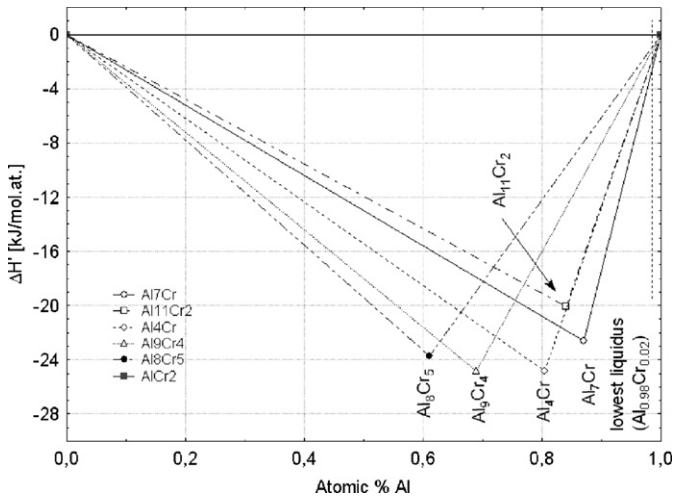

Fig. 6. Effective free energy of Al–Cr system formation. The point of intersection of dotted liquidus line and Al_7Cr line in top right corner represents the most negative formation enthalpy $\Delta H'$.

obtained points are connected to the end points of concentration axis, see Fig. 6.

The liquidus temperature of the Al–Cr binary system, when the greatest mobility and most effective mixing occurs, corresponds to 2 at.% of Cr, see Fig. 1, the element being in shortage at the interface where the Al–Cr compounds are formed. Because Al_7Cr has the most negative formation enthalpy $\Delta H' = -2.14$ kJ/mol at. ($\Delta H^0 = 13.4$ kJ/mol at., $C' = 2\%$ at $\sim 660\,^\circ$C and $C = 1/8$), it is expected to be the first phase formed in the diffusion zone.

In the case of the samples 7Al + Cr, two visible stops occur in cooling parts of the temperature profiles, evidencing phase transformations at the end of the synthesis process (Fig. 5b). The reaction $L + Al_{11}Cr_2 \rightarrow L + Al_7Cr$, marked as D, is inverse to the reaction at B. After this, in two-component diagram at a lower temperature, the eutectic reaction $L + Al_7Cr \rightarrow \alpha + Al_7Cr$ occurs, marked as E. So, it can be anticipated that the Al-based α solid solution will appear in the reaction product, as an unprocessed component.

XRD patterns for the 7Al + Cr samples show that the prevailing phase is Al_7Cr accompanied by some amount of Al_9Cr_4 and Al, see Fig. 7. Larger Cr particles result in larger quantity of unprocessed Al, with no residues of pure Cr. Some amount of Cr powder formed Al_9Cr_4 compound that probably at high temperature bonded finally

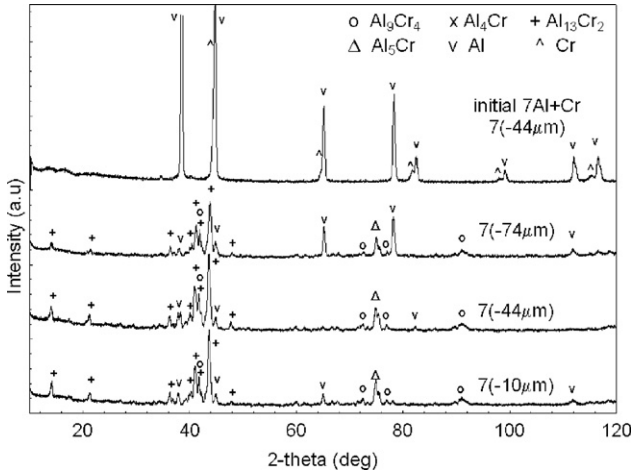

Fig. 7. XRD patterns of 7Al + Cr initial mixture and combustion products. Granularity changes of Cr powder (−10, −44 and −74 μm) induce relatively small changes in the product phase composition. $Al_{13}Cr_2$ composition corresponds to Al_7Cr.

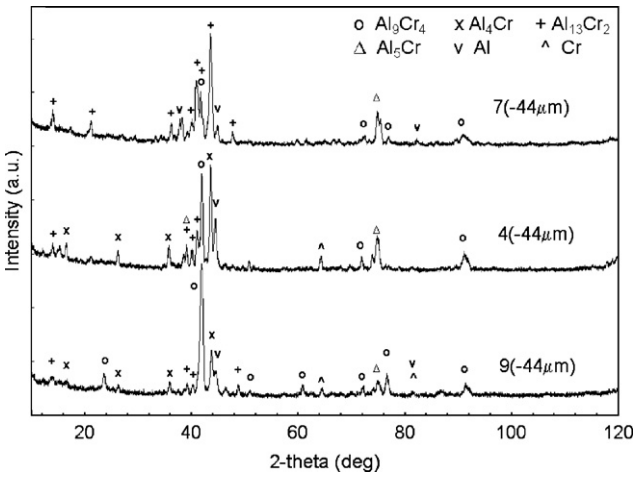

Fig. 8. XRD patterns of Al–Cr combustion products. Three compositions were mixed with identical granularity −44 μm with Al:Cr ratio 7:1, 4:1 and 9:4 (a/a). $Al_{13}Cr_2$ composition corresponds to Al_7Cr.

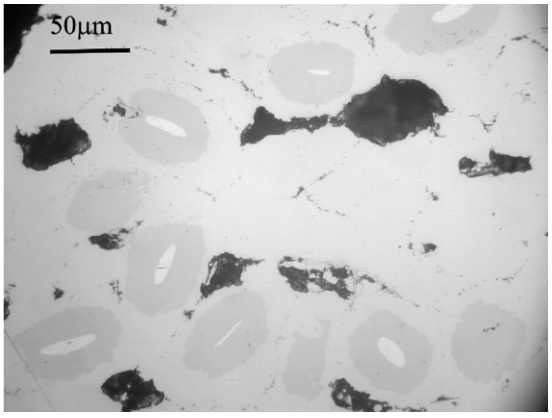

Fig. 9. Optical micrographs showing microstructure of a preform with large amount of unprocessed Cr powder ("cored" morphology).

the rest of Al and formed Al_7Cr. At the lowest granularity of Cr powder (−10 μm), the Al traces are small, which may be also a method to eliminate unprocessed Al. Unfortunately, this statement is contradicted by the eutectic transformation observed on the temperature diagram irrespective of Cr granularity.

Change of stoichiometric ratio of the initial mixture and increase of Cr content resulted in creating a mixture of other intermetallic compounds (Fig. 8). For the 4Al + Cr series, some other transient

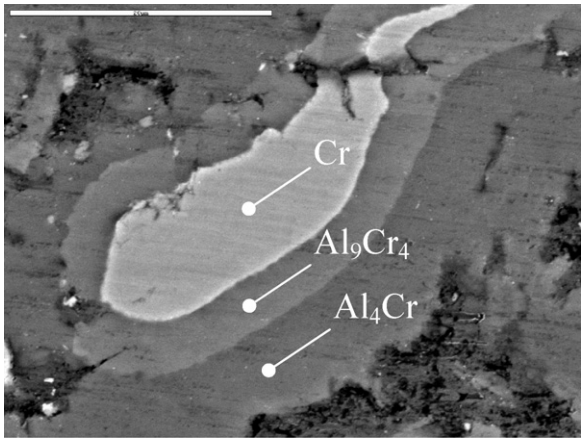

Fig. 10. Reaction zone around a partially reacted Cr particle.

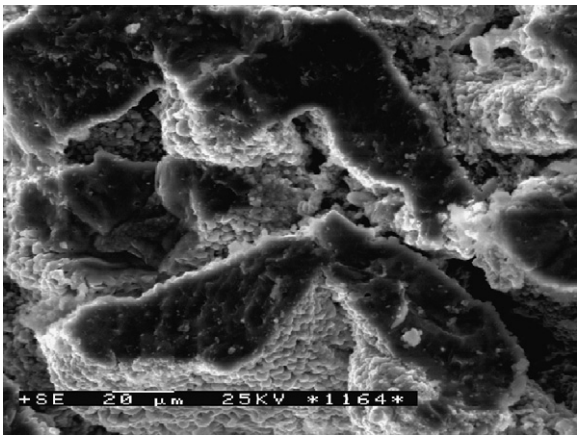

Fig. 11. Broken synthesis products: dark areas of Al–Cr compound covered with tiny particles.

phases occurred besides the clearly visible Al_4Cr. The presence of Cr is pronounced, which can prove incomplete processing of the initial powder. This phenomenon is especially intensive for the next 9Al + 4Cr samples with the largest Cr granularity of 74 μm. Smaller Al content and at the same time its shortage around the Cr particles probably slows down the reaction and results in "cored" morphology. This was confirmed by microscope observations together with chemical analysis.

The bright precipitate marked in Fig. 9, whose chemical composition was determined by EDS method (Fig. 10), is almost the initial Cr powder. During the synthesis, an envelope of Al_9Cr_4 forms around it, extending to the centre along with the reaction progress.

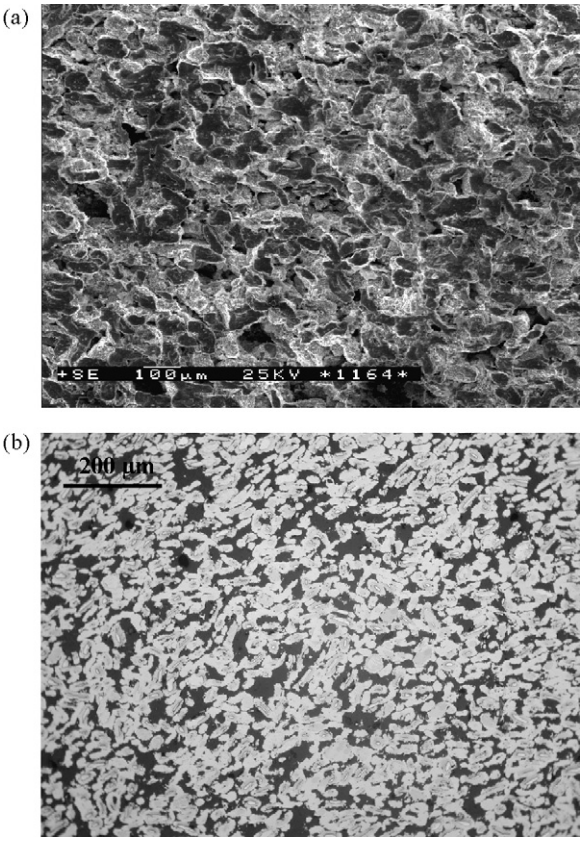

Fig. 12. Fracture of a preform produced from mixture of Al and Cr powders with stoichiometric ratio of 4:1 (4Al + Cr(−74 μm)) (a); microstructure of a porous 9Al + 4Cr(−74 μm) preform (b). Dark areas are pores filled with resin.

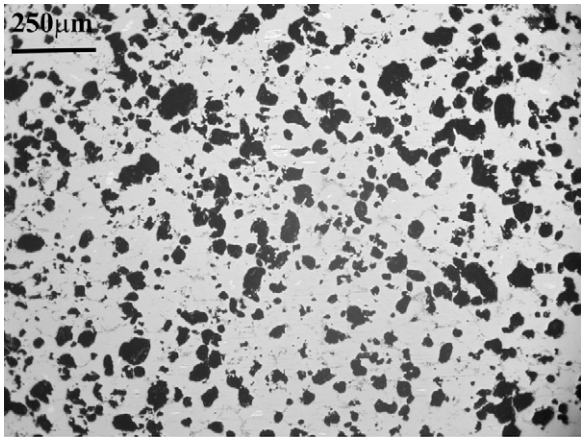

Fig. 13. Microstructure of a porous Al + 2Cr preform not approved for infiltration with aluminum alloy. Black spots are pores.

When the reaction is completed and the whole Cr powder bound, this compound is slowly decomposed and transformed to the compound earlier created outside, dominated by Al, Al_4Cr. When the Cr powder is more fine-grained or high temperature is maintained, the envelopes get dissolved and structure of the preform is uniform.

Microscopic observations of fractures revealed their characteristic structure, where the Al–Cr compounds created wavy formations, oblong and oval in cross-section. Their surface was spotted by tiny precipitates similar to cuboidal particles. The dark areas in Fig. 11 are fractured Al–Cr compounds, whose shape is probably related to Cr powder particles themselves.

Homogeneity of the obtained structures, as well as size and shape of the pores determine successful impregnation of a preform and quality of the composite. Fracture of the sample 4Al + Cr (Fig. 12a) shows uniform precipitates of Al–Cr compounds, separated by open gaps reaching deep inside the sample.

On the ground of fracture analysis, samples were selected to be impregnated by liquid aluminum alloy. Some materials, especially those with higher Cr content and thus obtained at higher synthesis temperature, were characterised by rounded pores with smooth walls, see Fig. 13. It was recognised that complete infiltration of such structures can be very difficult, so further works in this area were postponed.

The last stage of the works, among others to confirm suitability of the prepared preforms, was infiltrating them with liquid AlZn11Si2 alloy, together with analysis of the obtained microstructures. Using typical direct-squeeze casting parameters, a preform

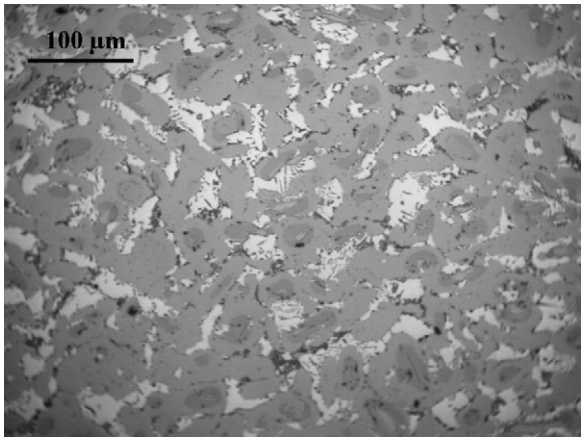

Fig. 14. Composite material obtained by infiltration of 9Al + 4Cr preform with casting aluminum alloy (light background).

before infiltration was heated to 500 °C and next casting was locally reinforced. Microscopic observations showed completely filled preform structure (Fig. 14), although in some cases small porosities occurred. There was never any displacement or segregation of the reinforcement. The structure was uniform and at this stage it seems that the prepared preforms could be infiltrated with liquid metal without greater difficulties. After infiltration, a porous and relatively hard preform should receive higher crack resistance and the reinforced zone should have proper physico-chemical properties.

4. Summary

The combustion synthesis (CS) method permits obtaining preforms built of intermetallic structures with porosity suitable for infiltration with liquid metal. The applied microwave energy intensifies the process, changes the heating way and allows forming the produced material structure. In the research, a special microwave chamber was applied in that radiation could be focused and the field distribution could be easily controlled depending on the charging material.

For the Al–Cr system, low enthalpy of forming intermetallic compounds requires preliminary heating of the initial powder mixture. Change of the stoichiometric ratio together with larger Cr content result in increased synthesis dynamics and temperature. For the 9Al + 4Cr samples, the recorded temperature changes show that synthesis proceeds through the peritectic transformations $L + Al_7Cr \rightarrow L + Al_{11}Cr_2 \rightarrow L + Al_4Cr$.

On the ground of differential thermal analysis and using the EHF model it can be ascertained that synthesis begins with formation of Al_7Cr that is transformed to a relevant compound according to contributions of the substrates. The reaction products comprise a few types of intermetallic compounds and, in some cases, unprocessed residues of the initial powders. When the Al content is large (7Al + Cr), free Al appears, whereas at higher Cr content (9Al + 4Cr) the remainder of Cr powder with typical "cored" structure is observed. This phenomenon is especially strong at the highest granularity of Cr powder, i.e. 74 μm. The produced materials are characterised by high open porosity, especially for the 9Al + 4Cr series, and can be used for infiltration with a liquid casting alloy.

Using the direct-squeeze casting method, the porous preforms were impregnated with casting aluminum alloy to reinforce the castings locally. Examinations of the composite structures revealed correct filling degree and satisfactory homogeneity of the preforms.

Acknowledgements

This work was subsidized by the Polish Ministry of Education and Science under the research project No. N508 054 31/2810.

References

[1] K. Morsi, Materials Science & Engineering A299 (2001) 1–15.
[2] J.J. Moor, H.J. Feng, Progress in Materials Science 39 (1995) 243–273.
[3] P. Mossino, Ceramics International 30 (3) (2004) 311–332.
[4] J.R. Jokisaari, S. Bhaduri, S.B. Bhaduri, Materials Science & Engineering A394 (2005) 385–392.
[5] E. Siores, D.D. Rego, Journal of Materials Processing Technology 48 (1–4) (1995) 619–625.
[6] D.K. Agrawal, Current Opinion in Solid State & Materials Science 3 (5) (1998) 480–485.
[7] S. Zhou, M.C. Hawley, Composite Structures 61 (4) (2003) 303–309.
[8] E.T. Thostenson, T.-W. Chou, Composites Part A: Applied Science and Manufacturing (Incorporating Composites and Composites Manufacturing) 30 (9) (1999) 1055–1071.
[9] J. Cheng, D. Agrawal, R. Roy, P.S. Jayan, Journal of Materials Processing Technology 108 (1) (2000) 26–29.
[10] M. Gupta, W.L.E. Wong, Scripta Materialia 52 (2005) 479–483.
[11] S. Aravindan, R. Krishnamurthy, Materials Letters 38 (4) (1999) 245–249.
[12] D. Atong, D. Clark, Ceramics International 30 (2004) 1909–1912.
[13] M. Audier, M. Durand-Charre, E. Laclau, H. Klein, Journal of Alloys and Compounds 220 (1995) 225–230.
[14] K. Mahdouk, J.-C. Gachon, Journal of Phase Equilibria 21 (2) (2000) 157–166.
[15] B. Gruszko, B. Przepiorzynski, E. Kowalska-Strzeciwilk, M. Surowiec, Journal of Alloys and Compounds 420 (2006) L1–L4.
[16] D. Vojtech, J. Verner, J. Serak, F. Simenacik, M. Balog, J. Nagy, Materials Science and Engineering A 458 (2007) 371–380.
[17] J.M. Torralba, V. Lancau, M.A. Martinez, F. Velasco, Journal of Material Science Letters 19 (2000) 1509–1512.
[18] M.R. Ali, A. Nishikata, T. Tsuru, Electrochimica Acta 42 (1997) 2347–2354.
[19] J. Creus, A. Billard, F. Sanchette, Thin Solid Films 466 (2004) 1–9.
[20] C.A. Handwerker, T.J. Foecke, J.S. Wallace, R.D. Jiggets, U.R. Kattner, Materials Science and Engineering: A 195 (June 1) (1995) 89–100.
[21] H. Faraoun, H. Aourag, C. Esling, J.L. Seichepine, C. Coddet, Computational Materials Science 33 (2005) 184–191.
[22] T. Chen, H.W. Chang, M.K. Lei, Nuclear Instruments and Methods in Physics Research, B 240 (3) (2005) 653–660.
[23] F. Zhang, W. Huang, Y.A. Chang, Calphad 21 (3) (1997) 337–348.
[24] K. Naplocha, A. Janus, J. Kaczmar, Z. Samsonowicz, Journal of Materials Processing Technology 106 (1–3) (2000) 119–122.
[25] C.L. Yeh, W.Y. Sung, Journal of Alloys and Compounds 384 (2004) 181–191.
[26] P. Mogilevsky, E.Y. Gutmanas, Materials Science and Engineering: A 221 (1–2) (1996) 76–84.
[27] R. Pretorius, Thin Solid Films 290–291 (1996) 477–484.
[28] C.C. Theron, R. Pretorius, O.M. Ndwandwe, J.C. Lombaard, Materials Chemistry and Physics 46 (2–3) (1996) 238–247.